

# Miscibility and Specific Interactions in Blends of Poly(*N*-vinyl-2-pyrrolidone) and Acid Functional Polyester Resins

Daniela Senatore,<sup>†,§</sup> Mark J. A. Berix,<sup>†</sup> Jozua Laven,<sup>†,\*</sup> Rolf A. T. M. van Benthem,<sup>†</sup> Gijbertus de With,<sup>†</sup> Brahim Mezari,<sup>‡</sup> and Pieter C. M. M. Magusin<sup>‡</sup>

Laboratory of Materials and Interface Chemistry and Schuit Institute of Catalysis, Eindhoven University of Technology, P.O. Box 513, 5600 MB Eindhoven, The Netherlands, and Dutch Polymer Institute (DPI), P.O. Box 902, 5600 AX Eindhoven, The Netherlands

Received January 4, 2008; Revised Manuscript Received September 4, 2008

**ABSTRACT:** Miscibility and intermolecular interactions of novel blends of poly(*N*-vinyl-2-pyrrolidone) (PVP) and acid functional polyester resins (APE) were studied by use of Differential Scanning Calorimetry (DSC), Attenuated Total Reflectance Fourier Transform Infrared (ATR-FTIR), Cross-Polarization Magic Angle Spinning (CPMAS) <sup>13</sup>C NMR spectroscopy and <sup>1</sup>H NMR relaxometry. The miscibility is found to be correlated to the number of acid end groups (acid value, AV) of APE and the molar mass (*M*) of PVP. Blends of APE with high AV and PVP with high *M* exhibit single-phase behavior in DSC and <sup>1</sup>H NMR. Both ATR-FTIR and <sup>13</sup>C NMR of these blends show composition-dependent displacements of the APE and PVP signals, which confirms that the two polymers are close together in the blend. In particular, FTIR spectra reveal a systematic blue shift of the stretch vibrations of both PVP and APE carbonyl groups. This indicates dipole–dipole interactions between a carbonyl group of PVP and a carbonyl of APE. The spectra contain a broad peak at about 1630 cm<sup>−1</sup>, which appears as a shoulder of the carbonyl stretch vibration of PVP. This band is ascribed to hydrogen bonding between the carbonyls of PVP and the hydrogen atoms of the end groups of the APE resins. Analysis of temperature-varied FTIR spectra of blends of PVP and a polyester resin of neopentyl glycol and isophthalic acid (PNI), used as a model of the APE resin, confirms the existence of such interactions.

## Introduction

The need for new polymer materials with controlled and tailored properties has driven the interest of industry and academia toward polymer blends, i.e., physical mixtures of two different homopolymers or copolymers. Blending two polymers provides new materials with a wide range of properties, depending on the type of constituents and their composition, without chemical synthesis of new polymers. A large number of polymer blends have been studied in the literature.<sup>1</sup> In general a miscible blend is the exception rather than the rule. However, if specific interactions such as dipole–dipole interactions, hydrogen bonding, charge transfer and acid–base interactions between the two constituents occur, then miscibility is observed.<sup>2</sup>

Poly(vinylpyrrolidone) (PVP) is a water soluble polymer, which is miscible with numerous polymers. The miscibility of PVP with hydroxyl-containing polymers like polyvinylalcohol,<sup>3–7</sup> poly(4-vinyl phenol),<sup>8</sup> poly(hydroxyether-bisphenol A),<sup>9,10</sup> and natural polymers<sup>11,12</sup> has been clearly attributed to hydrogen bonds between the carbonyl groups of the PVP (a H-acceptor) and the hydroxyl groups (a H-donor) of the other polymers. However, PVP has also been proved to be miscible with halogen-containing polymers like polyvinylchloride (PVC),<sup>13–15</sup> poly(chloromethyl methacrylate), poly(2-chloroethyl methacrylate),<sup>16</sup> poly(3-chloropropyl methacrylate), poly(2-bromoethyl methacrylate) and poly(2-iodomethacrylate).<sup>17</sup> For these blends, the miscibility is attributed to two kinds of intermolecular interactions: (1) dipole–dipole interactions between the carbonyl groups of the PVP and the carbon-halogen groups of the halogenated polymer; (2) H-bonding between the carbonyl groups of the PVP and the α-hydrogens of the

halogenated polymers (e.g., PVC). Fourier transform infrared (FTIR) study has shown that the stretch vibration of the PVP carbonyl groups shifts to higher frequency (blue shift). This shift has been ascribed to dipole–dipole interactions.<sup>14</sup> Moreover, Raman and solid-state NMR studies of the PVP/PVC blends confirmed the existence of dipole–dipole interactions, but no clear proof of hydrogen bonding was found.<sup>15</sup>

Blends of PVP with DL-poly lactide<sup>18</sup> have also been investigated. In this case hydrogen bonding interactions are not possible due the absence of H-donor groups. Nevertheless, the stretch vibration of the PVP carbonyl shows a shift to higher frequency. It was concluded that this shift cannot be ascribed to electric dipole–dipole interactions between the carbonyl groups of the PVP and those of the polyester, because the stretch vibration of the latter is independent of the PVP content.

In this study we describe, for the first time, blends of PVP with acid functional polyesters (APE) as used e.g. in powder coatings. Polyesters for such applications have typically low molar mass. They are synthesized by polycondensation of di- or trifunctional acids and alcohols with a functionality of two or higher. The functionality of these resins (i.e., carboxylic acid) is controlled by the monomer stoichiometry. For polyester formulations, carboxylic acid monomers normally include terephthalic acid, isophthalic acid, adipic acid and trimellitic anhydride, while the hydroxyl functional compounds are often aliphatic monomers such as neopentyl glycol, ethylene glycol, and trimethylolpropane.<sup>19</sup> In the curing step of a powder coating, the polyester thermosets by reacting with a suitable cross-linker. Our interest to blends of PVP and APE derives from the use of PVP as the encapsulant of a powder coating cross-linker.<sup>20</sup> The miscibility of PVP with the APE resins plays an important role in the mechanism of release of the cross-linker upon curing of the powder coating formulation.

For that reason, we characterized the miscibility of blends of PVP and APE by measuring the glass transition with differential scanning calorimetry (DSC) and <sup>1</sup>H spin–lattice

\* Corresponding author. E-mail: j.laven@tue.nl. Telephone: +31(0)402473682. Fax: +31(0)40244 5619.

<sup>†</sup> Laboratory of Materials and Interface Chemistry, Eindhoven University of Technology.

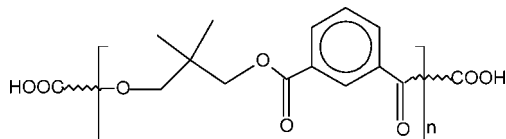
<sup>‡</sup> Dutch Polymer Institute.

<sup>§</sup> Schuit Institute of Catalysis, Eindhoven University of Technology.

**Table 1. Monomer Composition and Properties of the Acid-Functional Polyester**

resin	monomer (mol %)						AV (mg KOH/g)	$M_n$ (g/mol)	$M_w/M_n$
	NPG <sup>a</sup>	TPA <sup>b</sup>	IPA <sup>c</sup>	EG <sup>d</sup>	AA <sup>e</sup>	TMA <sup>f</sup>			
APE-1	40	40		5	5	10	75	2982	2.2
APE-2	45	45	5		5		24	5710	2.0
PNI	50		50				30	4723	1.8

<sup>a</sup> Neopentyl glycol. <sup>b</sup> Terephthalic acid. <sup>c</sup> Isophthalic acid. <sup>d</sup> Ethylene glycol. <sup>e</sup> Adipic acid. <sup>f</sup> Trimellitic anhydride.

**Figure 1.** Acid functional polyester resin of neopentylglycol and isophthalic acid (PNI).

relaxation with  $^1\text{H}$  NMR. In addition, we investigated the specific interactions between the two polymers with FTIR and cross-polarization (CP) magic angle spinning (MAS)  $^{13}\text{C}$  NMR spectroscopy. We will show that both dipole–dipole interactions and H-bonds are observable in this system. Finally, we measured the length scale of miscibility via spin diffusion measurements.

## Experimental Section

**Materials.** Polyvinylpyrrolidone was obtained from Aldrich and used without further purification. Three types of PVP of different weight averaged molar mass ( $M_w$ ) were used: PVPK15 (10000 g/mol), PVPK30 (40000 g/mol) and PVPK90 (360000 g/mol). Acid-functional polyester resins (APE-1, APE-2 and PNI) were obtained from DSM Resins BV (Zwolle, NL). Chloroform ( $\text{CHCl}_3$ ), tetrahydrofuran (THF), and *N*-methyl-2-pyrrolidone (NMP) were purchased from Aldrich and were used as supplied.

**Characterization of Carboxylic Acid–Functional Polyester Resins.** The chemical composition, the concentration of the acid groups (acid value, AV) and the molar masses of APE-1, APE-2 and PNI resins were determined by  $^1\text{H}$  NMR spectroscopy in solution, by titration and by Gel Permeation Chromatography (GPC) respectively. Solution  $^1\text{H}$  NMR was performed on a Varian Mercury VX 400 MHz spectrometer with deuterated chloroform as the solvent. The monomer composition of each resin was determined by integration of the  $^1\text{H}$  NMR signals. Potentiometric titrations were carried out using a Metrohm Titrino 785 DMP automatic titration device fitted with an Ag electrode. A known amount of the resin was dissolved in *N*-methyl-2-pyrrolidone. This solution was titrated with a solution of potassium hydroxide (KOH) of concentration 0.1 M. The AV is expressed as milligrams of KOH required to neutralize the carboxylic acid contained in one gram of resin.

GPC was carried out using a Waters GPC apparatus, equipped with a Waters 510 pump and a Waters 410 refractive index detector at 40 °C. Two linear columns, mixed C, Polymer Laboratories, 30 cm, 40 °C, were used. Tetrahydrofuran (THF) was used as the eluent at a flow rate of 1.0 mL/min. Calibration curves were obtained using polystyrene standards (Polymer Laboratories,  $M = 580$  g/mol to  $M = 7.1 \times 10^6$  g/mol). Data acquisition and processing were performed using Waters Millennium32 (v3.2 or 4.0) software.

Table 1 shows the monomer compositions, the acid values and information on the number (*n*) and weight (*w*) averaged molar masses of the APE resins used. The APE-1 is a branched resin, due to the presence of trimellitic anhydride (TMA), while APE-2 and PNI have a linear structure. Moreover, APE-1 has a higher acid value than the other two resins. Although the main components of both resins are neopentyl glycol and terephthalic acid, the presence of small amounts of other monomers makes the structure of those resins rather complex to be studied via solid state NMR. For this reason, we also studied the linear acid-functional resin (Figure 1) which is composed only of neopentyl glycol and

isophthalic acid (PNI), as a model resin to investigate the interactions between the PVP and the APE resins via solid state NMR.

**Preparation of the Blends.** All blends of PVP and CPE were prepared by solution-casting. First, the PVP and the APE resin were mixed on weight basis in different proportions. Then, the resulting powder mixtures were dissolved in a solution of THF and  $\text{CHCl}_3$ . The total concentration of the two polymers in solution was 10% by weight (wt %). The solutions were stirred for 20 min at 55 °C until a transparent solution was obtained. The solutions of the pure polymers and blends were cast in aluminum cups. To allow the solvent to evaporate, the castings were dried at 60 °C in a vacuum oven for about 1 day. The castings were kept in a desiccator containing silica gel to minimize contact with the atmospheric moisture until further characterization. In the case of PVP/PNI blends, only  $\text{CHCl}_3$  was used as solvent with a total polymer concentration of 10 wt %. The solution was then subjected to the same treatment as described above. The composition of the polymer blends ranged from 10 to 90 wt % of PVP.

**Characterization of the Blends.** The DSC measurements were performed with a Perkin-Elmer Pyris 1 calorimeter, calibrated with indium and lead standards. The samples were placed in aluminum pans of 50  $\mu\text{L}$  with a pinhole in the lid. The sample weights varied between 18 and 22 mg. The samples were first heated from –30 °C up to 170 °C at 20 °C/min and annealed at 170 °C for 5 min to allow the residual water to evaporate and to enhance the contact of the samples with the aluminum pans. Then, the samples were cooled down to –30 at 30 °C/min and finally they were heated up to 230 at 20 °C/min. All runs were performed under nitrogen flow. The glass transition temperatures  $T_g$  of the polymer blends were calculated as the midpoint of the heat capacity jump of the second heating.<sup>21</sup>

ATR-FTIR was performed using a Bio-Rad Excalibur infrared spectrometer equipped with an ATR diamond unit (Golden Gate). The spectra were recorded at room temperature, with 2  $\text{cm}^{-1}$  resolution, by averaging 50 scans in the range 4000–650  $\text{cm}^{-1}$ . Moreover, the blends of PNI/PVP containing 10 wt %, 20 wt %, and 30 wt % of PVP were also analyzed at temperatures ranging from 50 to 170 °C. In these experiments, the blends were heated up to 170 °C under nitrogen flow and annealed for 15 min at this temperature to allow any residual water to evaporate. The temperature was progressively reduced and spectra of the samples were acquired between 170 °C and 50 °; this took approximately 45 min in total.

Cross-polarization magic angle spinning (CPMAS)  $^{13}\text{C}$  NMR spectra were recorded at room temperature on a Bruker DMX500 spectrometer equipped with a 4-mm MAS probe head and operating at  $^{13}\text{C}$  and  $^1\text{H}$  NMR frequencies of 125 and 500 MHz, respectively. The sample rotation rate of 10 kHz was carefully chosen to avoid overlap of spinning sidebands. The 90° pulse for both  $^1\text{H}$  and  $^{13}\text{C}$  was 5  $\mu\text{s}$ .  $^{13}\text{C}$  NMR spectra were obtained under high-power proton decoupling with an interscan delay of 3 s and a CP contact time of 3 ms. Typically 4096 scans were recorded. The adamantane peak at 38.56 ppm was used as an external reference for the chemical shift.  $^1\text{H}$  NMR spin–lattice relaxation in the laboratory and rotating frame,  $T_1$  and  $T_{1\rho}$ , were recorded under static conditions with an interscan delay of 5 s.  $T_1$  was measured by use of an alternated inversion–recovery pulse sequence  $(90^\circ)_{+x}-(90^\circ)_{\pm x}-\tau-(90^\circ)_\phi$ –acquisition and  $T_{1\rho}$  by use of a spinlock sequence  $(90^\circ)_\phi-(v_\rho)_\phi$ –90 acquisition with variable spin-lock pulse duration  $v_\rho$ .

## Results and Discussion

**DSC Analysis.** Blends were composed by mixing one out of three poly(vinyl pyrrolidone)s, grades PVPK15, PVPK30 and PVPK90 (with molar masses 10, 40 and 360 kg/mol), with either a commercial acid-functionalized polyester resin (APE-1 or APE-2, with acid values 1.4 and 0.4 mmol/g) or a PNI, a well defined alternating copolymer of neopentylglycol and isophthalic acid (acid value 0.4 mmol/g). APE-1 is a branched resin, due to the presence of trimellitic anhydride (TMA), while APE-2 and PNI have a linear structure. The results of the DSC

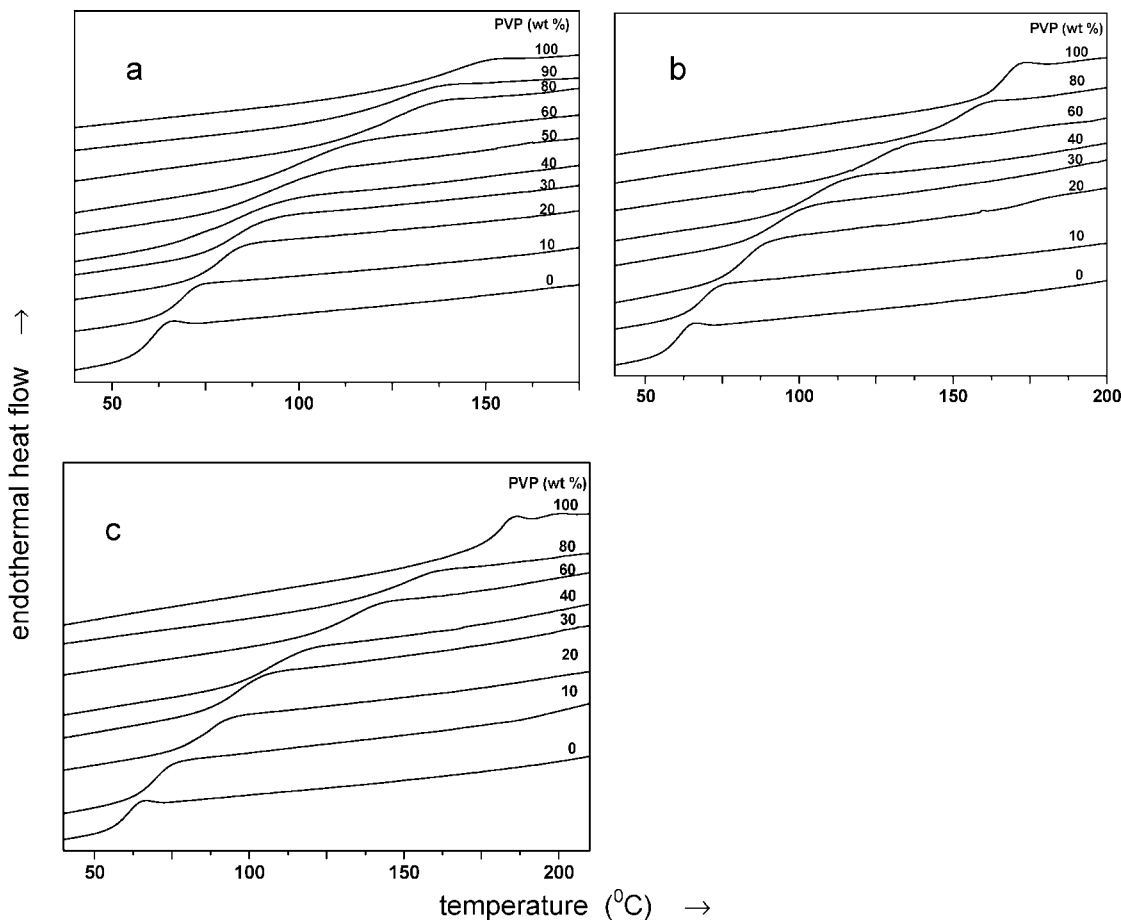


**Figure 2.** DSC thermograms of APE-1 blended with PVPK15 (a), PVPK30 (b), and PVPK90 (c). The number associated to each curve refers to the weight percentage of PVP.

measurements of the blends of the acid functional polyester APE-1 with PVP of different molar masses are shown in Figure 2. The weight percentages range from pure PVP (top curve) to pure APE-1 (bottom curve). Note that annealing for 5 min at 170 °C prior to the measurement should also be sufficient to remove any residual solvent trace. A single glass transition was observed for all APE-1/PVP blends at temperatures between the  $T_g$  values of the component polymers, which is an indication of a miscible blend.<sup>22</sup> A nonmiscible blend would show two  $T_g$  values corresponding to the  $T_g$  values of the individual components. However, the observation of a single  $T_g$  in DSC does not necessarily mean that the two polymers are mixed at a molecular level. Indeed, a particular blend may be characterized as miscible with one technique and immiscible with another.<sup>23</sup> The limit of resolution inherent to the technique used permits an estimation of the upper limit of the scale of miscibility. The  $T_g$  measured by DSC is sensitive to heterogeneities with sizes of about 25–30 nm and larger.<sup>24</sup>

Several attempts to relate the  $T_g$  of a miscible blend to its composition have been reported in literature.<sup>25</sup> Two of the most well-known equations are the Fox equation<sup>26</sup>

$$\frac{1}{T_g} = \frac{w_1}{T_{g1}} + \frac{w_2}{T_{g2}} \quad (1)$$

and the Gordon–Taylor equation,<sup>27</sup>

$$T_g = \frac{(w_1 T_{g1} + k w_2 T_{g2})}{(w_1 + k w_2)} \quad (2)$$

where  $w_i$  ( $i = 1, 2$ ) is the weight fraction of the blend component  $i$ ,  $T_{gi}$  ( $i = 1, 2$ ) is the glass transition temperature, in Kelvin, of

component  $i$  and  $T_g$  is the glass transition temperature of the mixture. The parameter  $k$  is defined by

$$k = \frac{V_2 \Delta \alpha_2}{V_1 \Delta \alpha_1}$$

where  $\Delta \alpha_i$  is the change in cubic thermal expansion coefficient of the  $i$ th component at its glassy transition temperature and  $V_i$  its specific volume. In practice,  $k$  is often determined as an adjustable fit parameter for the composition dependence of  $T_g$ . E.g.,  $k = 1$  corresponds to the linear case whereas  $T_g$  is the weighed-average of the respective homopolymer values.

Figure 3 shows the  $T_g$  versus the composition of the PVP/APE-1 blends. The Fox equation fits the  $T_g$  versus composition data of the blend of APE-1 with the lowest molar mass PVP well. By increasing the molar mass of PVP, a slight, positive deviation from the Fox equation is observed. This result suggests that specific interactions between the two polymers are responsible for their miscibility. In addition, the Gordon–Taylor equation seems to predict the  $T_g$  versus composition data of the blends of APE-1 with all PVPs very well. The adjustable parameter  $k$ , which was calculated with a least-squares method, is close to unity in all cases, indicating that the specific interactions between the two components are not very strong. Many examples of miscible blends which have a strong deviation from the Fox and Gordon–Taylor equations have been reported. In these studies, the miscibility is attributed to H-bond interactions between the H-donor groups of one of the polymeric constituents and the H-acceptor groups of the other constituent. An example is the mixture of a H-donor polymer like poly(4-vinylphenol) with a H-acceptor polymer like PVP.<sup>8</sup> The type of interaction is not only strong but the number of interactions

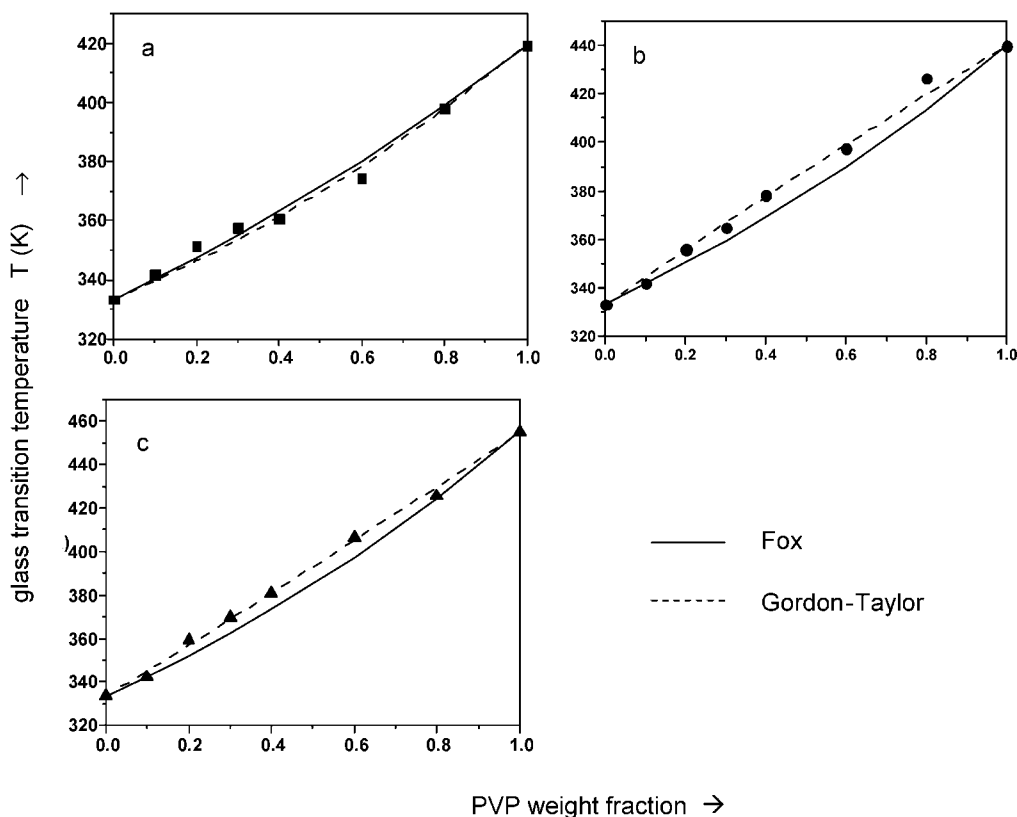


**Figure 3.** Composition dependence of  $T_g$  blends of APE-1 with PVPK15 (a, ■), PVPK30 (b, ●), and APE-1/PVPK90 (c, ▲) with fit curves based on the Fox equation, eq 1 (continuous line), and the Gordon–Taylor equation, eq 2, with  $k = 0.93$ , 1.00 and 0.99 in a, b, and c, respectively (broken line).

is also high, because it involves a group of the repeating units of the two polymers.

The second type of resin (APE-2) demonstrates a different behavior compared to APE-1. Figure 4a shows the DSC traces of the blends of APE-2 with the lowest molar mass PVP (i.e., PVPK15). Up to 20 wt % in PVP, the DSC curves show the single-phase behavior which we have also seen for the APE-1/PVP blends. A single glass transition is observed at a temperature between the  $T_g$  values of pure APE-2 and PVPK15. At 30 wt % in PVP, the DSC curve still seems to reflect a single  $T_g$  temperature but its value remains similar to that of the 20 wt % PVP blend. At 40 wt % PVP, the DSC trace shows clearly two  $T_g$  transitions (Figure 4, parts a and d) and at 60 wt % PVP one broad  $T_g$  is noticeable. Finally, the thermogram of the blend containing 80 wt % of PVPK15 displays again one  $T_g$ , which is very close to that of the pure PVP.

For comparison, a single  $T_g$  transition is observed at each composition for the blends of APE-2 with the higher molar mass PVPK30 (Figure 4b). The glass transition of the blend with 60 wt % PVP is much broader than the glass transition of the pure polymers and the other of APE-2/PVPK30 blends. Such broadening is indicative of partial miscibility.<sup>28</sup> Finally, the blends of APE-2 with the highest molar mass PVPK90 exhibit a single glass transition for all compositions (Figure 4c). Moreover, the width of the transitions of the 40/60 and 60/40 APE-2/PVPK90 blends is smaller than that of the corresponding blends with PVPK30. All these observations suggest that the miscibility of PVP with APE-2 improves by increasing the molar mass of the PVP.

How are we to explain this behavior? It is known that solution mixing of polymers can produce nonequilibrium blends and that a miscible pair can form a two phase structure depending on the type of solvent used and the method of solvent evaporation.

A method to test whether this is a possible cause of the apparent immiscibility of the blends of APE-2 with PVPK15 and PVPK30, is to use an extensive annealing step or a different solvent and see if this affects the result. If the immiscibility of a blend is the result of a nonequilibrium situation, then, after sufficient annealing, the DSC trace of that sample should show only one  $T_g$ .<sup>29</sup> The much more extensive annealing was done in the DSC by 4 cycles of heating to 200 °C, holding at 200 °C for 5 min and cooling down to –30 °C, at rates of 20 °C/min. Figure 4d shows DSC curves of this thoroughly annealed blend with 40 wt % PVP, and of a blend with the same composition cast from a different solvent, *N*-methyl-2-pyrrolidone, without extensive annealing. The DSC curves still exhibit two  $T_g$  values, even more distinct. Therefore, we can conclude that the immiscibility shown by the blend of APE-2 with the lowest molar mass PVP in the composition range of 30 to 60 wt % PVP is not an artifact, caused by kinetics. In the next section the type of interactions in the blends will be investigated in order to explain the (im)miscibility of blends with APE-2.

Figure 5 shows the composition dependence of  $T_g$  for the miscible blends of APE-2 with PVPK30 and PVPK90. For APE-2/PVPK30 blends the  $T_g$ s at 60 and 80 wt % of PVPK30 deviate from both the Fox and Gordon–Taylor relations (eqs 1 and 2). Such positive deviation can be caused by strong specific interactions between the two constituents. In contrast, for the APE-2/PVPK90 blends the relation between  $T_g$  and composition blends is well described by the Fox and Gordon–Taylor equations.

In Figure 6a the DSC traces are plotted and in Figure 6b the composition dependence of  $T_g$  is given for the blends of the resin PNI with the PVP of intermediate molar mass, PVPK30. Similarly to the blend of APE-1 with PVP, the DSC data show a single  $T_g$  at all compositions and the experimental data are



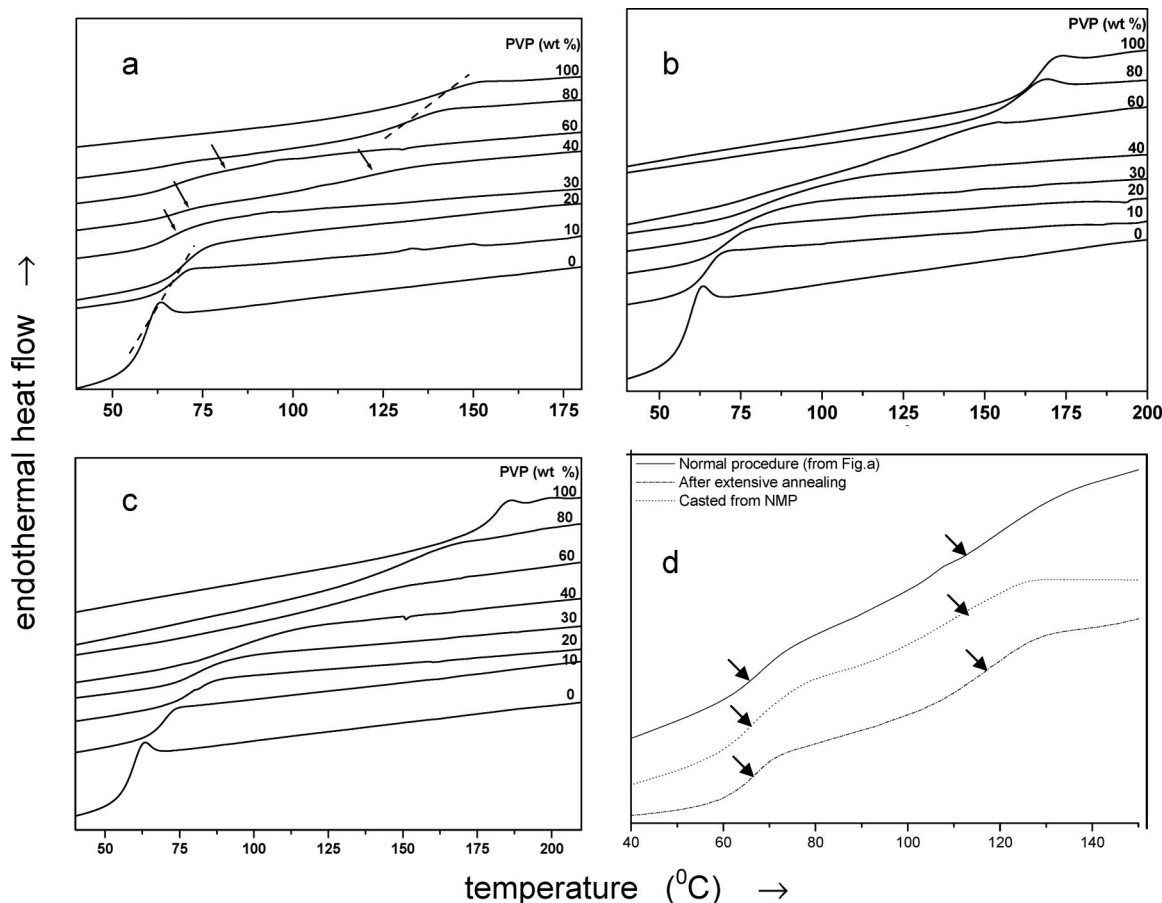


**Figure 4.** DSC thermograms of APE-2 blended with (a) PVPK15, (b) PVPK30, and (c) PVPK90 after the standard annealing procedure and (d) of APE-2 with 40 wt % PVPK15, after extensive annealing in the DSC furnace (dashed line) and after standard annealing but casted from a different solvent, *N*-methyl-2-pyrrolidone (NMP, line with fine dots). The curves have been displaced vertically to separate them from each other. Arrows indicate the two phase transitions observed for blends with PVPK15.

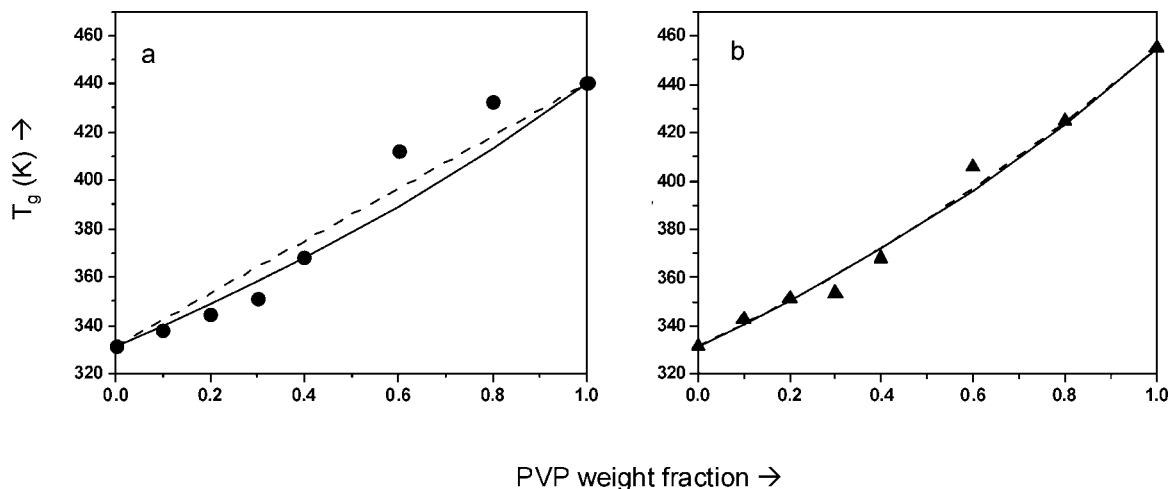


**Figure 5.** Composition dependence of  $T_g$  for miscible blends of APE-2 with (a) PVPK30 (●) or (b) PVPK90 (▲). Curves are based on eqs 1 (continuous) and 2 (broken; with  $k = 1.0$  and  $0.9$ , respectively).

perfectly represented by both the Fox and the Gordon–Taylor equations.

**FTIR Analysis.** The use of infrared spectroscopy to characterize polymer miscibility is well-known, particularly when a polymer contains carbonyl groups (e.g., polyesters and polycarbonates)<sup>23</sup> If two polymers form completely immiscible blends, there should be no appreciable change in the IR spectrum of the blends with respect to each component spectrum. If mixing occurs on a molecular scale, the local environment of

the carbonyl groups may be perturbed sufficiently to cause a displacement of the frequency of the carbonyl stretch absorption by as much as  $20\text{ cm}^{-1}$ . A spectral shift of this magnitude may reasonably be taken as evidence that a specific interaction (e.g., hydrogen bonding) occurs between the carbonyl group and the second polymer.

Figure 7 shows the IR spectra of APE-1, APE-2, PVPK15, PVPK30, PVPK90 and their blends, in the region from  $1500\text{ cm}^{-1}$  to  $2000\text{ cm}^{-1}$ . The spectra of the pure PVPs show a band

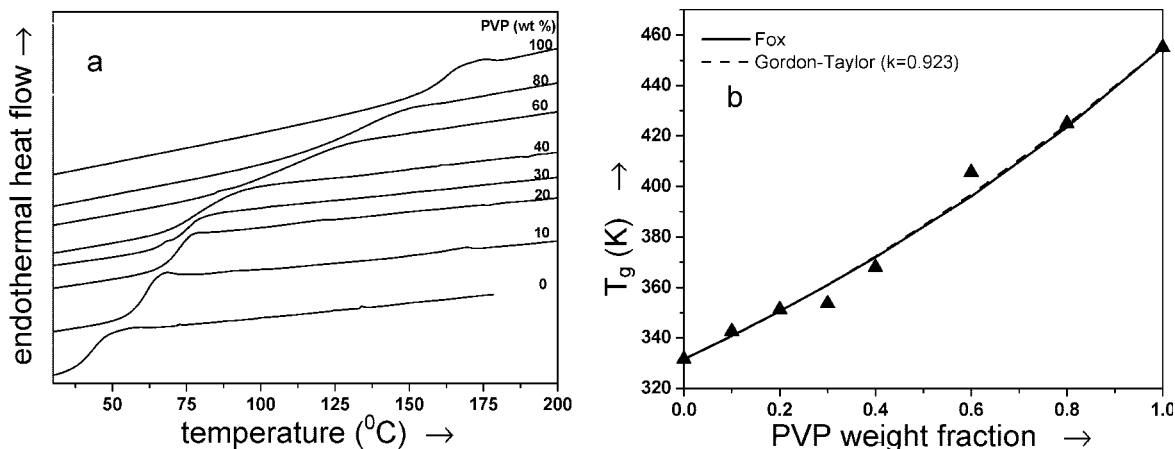


**Figure 6.** (a) DSC thermograms of PNI and PVPK30 blends with labels indicating the weight percentage of PVP and (b) composition dependence of  $T_g$  for PNI/PVPK30 blends with fit model based on eqs 1 (continuous) and 2 (broken; with  $k = 0.923$ ).

at about  $1656\text{ cm}^{-1}$  which is assigned to the  $\text{C}=\text{O}$  stretching vibrations of the amide group. The fact that this band is significantly broadened could be indicative of strong intermolecular and intramolecular interactions between the amide groups of the PVP.<sup>30</sup> Upon adding the carboxylic acid functional polyesters, this band shifts to higher frequencies by about  $25\text{ cm}^{-1}$  (blue shift). The blue shift cannot be attributed to the formation of hydrogen bonds as this would decrease the stretching vibration of the carbonyl, giving a shift to lower frequency (red shift). A blue shift of the carbonyl of the amide group of the PVP was previously observed in blends of PVP with polyvinylchloride<sup>15</sup> (PVC) and DL-poly lactide<sup>18</sup> (PLC). For the PVP/PVC blend, it was suggested that dipole–dipole interaction between the amide  $\text{C}=\text{O}$  of the PVP and the  $\text{C}-\text{Cl}$  bond of the PVC was the major reason for the observed shift. However, those authors conclude that the presence of hydrogen bonds between the carbonyls of the PVP and the  $\alpha$ -hydrogens of the PVC was too weak to be visible.

For the PVP/PLC blends, those authors attributed the blue shift of the PVP carbonyl to the elimination of strong intermolecular and intramolecular interactions in PVP, upon mixing with PLC. They concluded that dipole–dipole interactions between the  $\text{C}=\text{O}$  of the PVP and the  $\text{C}=\text{O}$  of the PLC were not present as the wavenumber of the latter group did not show any shift upon blending with PVP. In contrast, we observed that the polyester carbonyl stretching band, in the pure polyester resin at  $1715\text{ cm}^{-1}$ , shifts to higher frequencies upon increasing the amount of PVP from 10 to 90 wt %. This blue shift (about  $5\text{ cm}^{-1}$ ) is much smaller than the blue shift by about  $25\text{ cm}^{-1}$  for the PVP carbonyl band (at  $1715\text{ cm}^{-1}$  in pure PVP). It appears that in the pure PVP as well as in the pure resin, dipole–dipole interactions between carbonyls exist. Upon blending the two polymers together, part of these specific PVP–PVP and resin–resin interactions are broken, but new interactions appear between a carbonyl of the PVP and a carbonyl of the polyester resin. These new interactions are also dipole–dipole interactions and, therefore, will have a strength similar to the corresponding interactions in the pure polymer. This interpretation is in agreement with the  $T_g$  versus composition behavior. Indeed, the good fitting of the experimental data with the Fox and Gordon–Taylor ( $k = 1$ ) equations shows that the interactions which are formed between the PVPs and the APEs are of similar strength of the interactions existing between macromolecules of the pure polymers.

The IR spectra of all the blends show a new band at about  $1630\text{ cm}^{-1}$ , as a shoulder to the normal  $\text{C}=\text{O}$  band of pure PVP. This band is very broad and becomes clearly visible at the lowest content of PVP. Moreover, the intensity of this shoulder is

approximately constant between 10 and 40 wt % of PVP. A possible explanation for the appearance of this shoulder is the formation of H-bonds between the carbonyls of the PVP and the acid end-groups of the carboxylic acid functional polyesters. As noted before, the occurrence of H-bonding between the carbonyl of the PVP and a hydrogen donor group (i.e., OH or COOH) causes a shift of the carbonyl stretching band to lower frequencies. In blends of PVP with polymers which have a repeating unit containing a hydrogen donor like OH (e.g., poly(vinylphenol), PVPh), Moskala et al. found a clear shoulder on top of the amide carbonyl band due to the presence of both “free” and H-bonded carbonyls.<sup>8</sup> They showed that the intensity of the stretching band of the H-bonded carbonyl increases with increasing amount of PVPh. In our case, the broad band at  $1630\text{ cm}^{-1}$  has a low intensity which remains constant by increasing the amount of PVP from 10 to 40 wt %. This result can be explained if we consider that the acid groups of the APE resins, which can interact via H-bonding with the carbonyls of the PVP, are end-groups. If we calculate the number of acid groups of the resin and the number of carbonyl groups of PVP of a blend containing 10 wt % of the latter, it becomes clear that the number of proton acceptor groups is about 100 times higher than the number of proton donor groups. Consequently, only a small amount of carbonyl groups of PVP can form H-bonds with the acid end-groups of the APE. It is clear that the number of acid end-groups that forms H bonds with a carbonyl of PVP is already saturated at the lowest content of PVP. Therefore, the intensity of the H-bonded carbonyl stretching is very low and does not rise upon increasing the amount of PVP. This broad band at  $1630\text{ cm}^{-1}$  cannot be discerned anymore from the main carbonyl band in the mixture with the highest content of PVP (80 wt %).

In order to confirm that the broad band at  $1630\text{ cm}^{-1}$  is due to the stretching of the PVP carbonyl groups which are H-bonded to the acid end-groups of the resins, we measured the IR spectra of the blend of PNI and PVPK30 over a range of temperatures. It is known that the number of hydrogen bonds decreases with increasing temperature, due to prevailing entropic contributions.<sup>31</sup> For example, He et al.<sup>32</sup> reported that the fraction of carbonyl groups associated through H-bonding, in blends of poly( $\epsilon$ -caprolactone) (PLC) and 4,4′-thiophenol (TDP), decreases on increasing the temperature. On the basis of IR spectra of the blends between 26 and  $160^\circ\text{C}$ , these authors clearly showed that the stretching of the carbonyl of PLC, which is H-bonded, decreases in intensity and shifts to higher frequencies with the increase of the temperature. Figure 8 shows the IR spectra in the region  $1600\text{--}1800\text{ cm}^{-1}$  of pure PNI and its blends with 10, 20, and 30 wt % of PVPK30. The spectra were

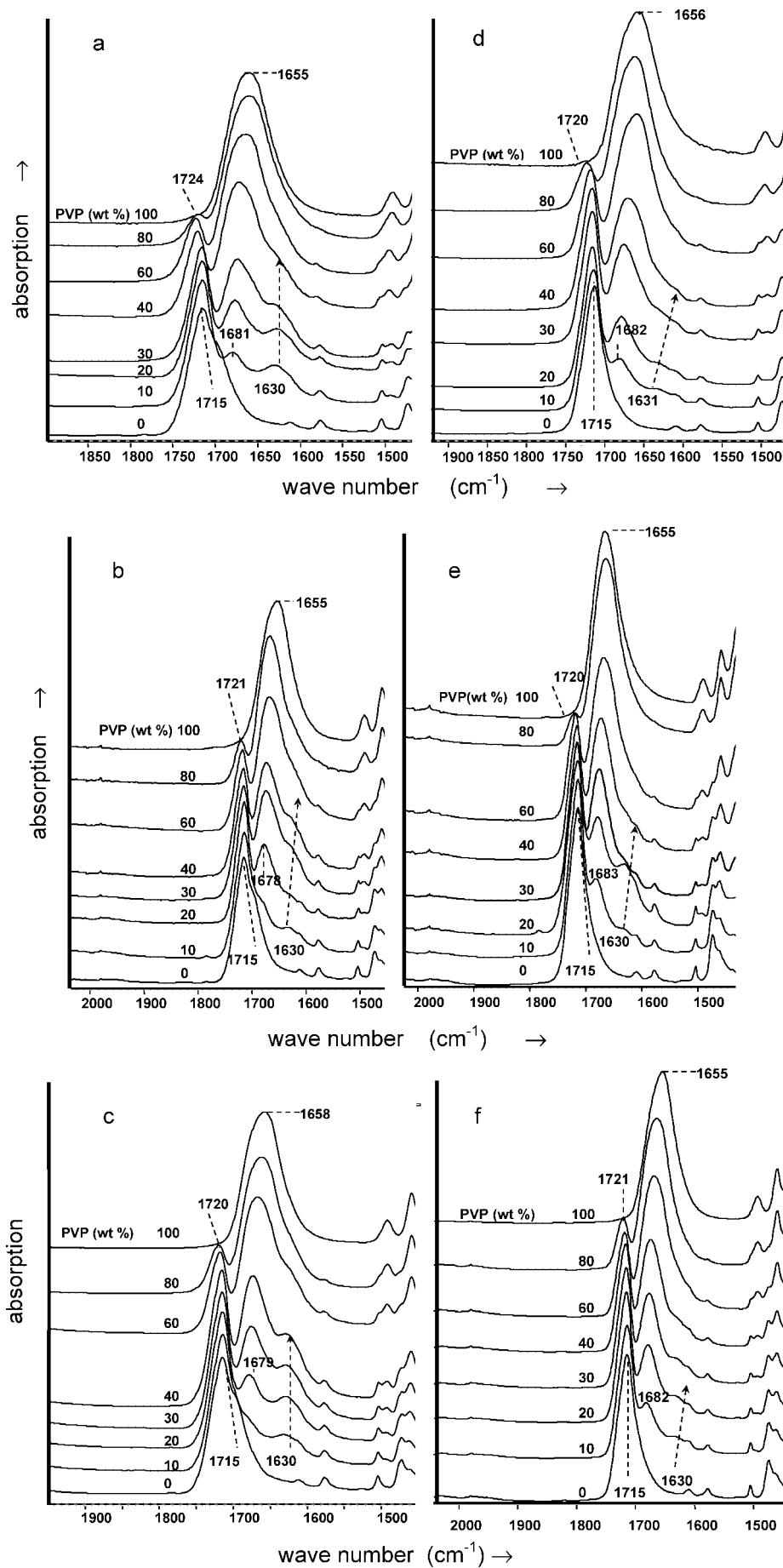


**Figure 7.** Infrared spectra of APE-1 blended with PVPK15 (a), PVPK30 (b), and PVPK90 (c) and of APE-2 blended with PVPK15 (d), PVPK30 (e), and PVPK90 (f).

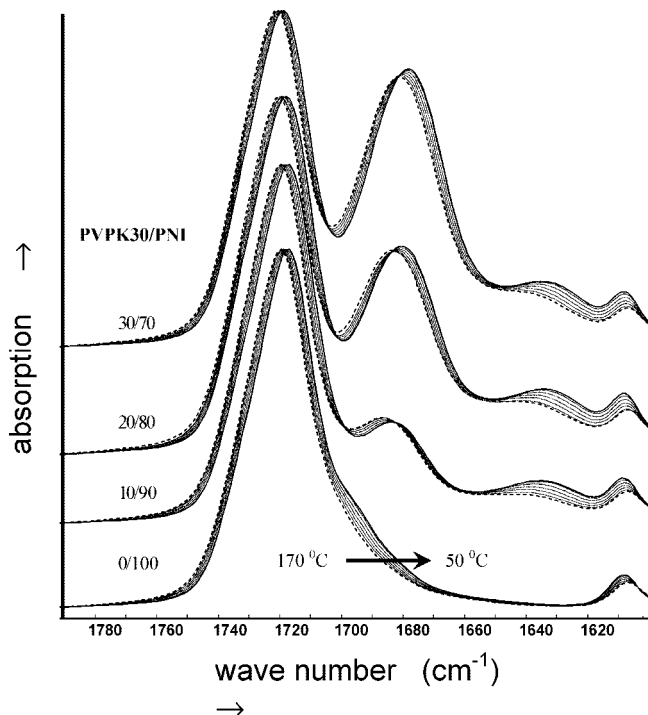


**Figure 8.** Infrared spectra of PVPK30/PNI blends upon decreasing the temperature from 170 °C (--) to 50 °C (—) with intermediate temperatures 150, 130, 120, 90, and 70 °C. The numbers associated with each group of curves refer to the weight percentage of PVP.

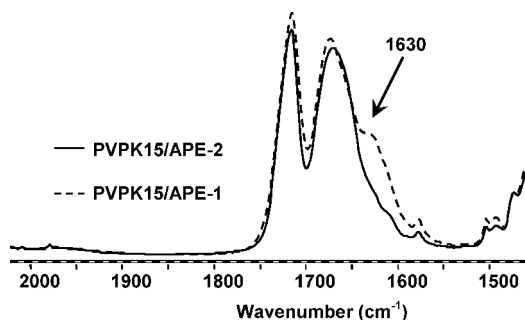


**Figure 9.** ATR-FTIR spectra of 40 wt % PVPK15 with APE-1 (dashed line) and APE-2 (continuous line).

recorded at different temperatures. For each composition, spectra are shown at 50, 70, 90, 110, 130, 150, and 170 °C. For all the blends containing the PVP, the intensity of the broad band at about 1630  $\text{cm}^{-1}$  decreases and at the same time shifts to higher frequency. These results confirm that this band is due to the stretching of H-bonded carbonyls of PVP. Because the acid end-groups are the only groups of the APEs which can donate hydrogen, we conclude that, besides the dipole–dipole interactions, also H-bonds between PVP and APE exist.

Qualitatively, the FTIR spectra of the blends of APE-2 with the lowest molar mass PVP show the same features as the other, miscible blends, i.e. a shift of the PVP carbonyl peak to higher frequency upon blending and the appearance of a broad peak at a lower frequency. However, if we compare the spectra of APE-2/PVPK15 with those of APE-1/PVPK15 (Figure 7, parts a and b), we see that the broad peak at about 1630  $\text{cm}^{-1}$  is much weaker for the former. This effect is even more clear in Figure 9 which shows the FTIR spectrum of the “immiscible” 40/60 PVPK15/APE-2 with the “miscible” 40/60 PVPK15/APE-1. The latter has a clear peak at about 1631  $\text{cm}^{-1}$ , while for the former a rather weak shoulder of the PVP carbonyl is observed. As we have attributed the peak at 1631  $\text{cm}^{-1}$  to the H-bonds

between COOH end-groups of the APEs and carbonyls of the PVP, we conclude that these types of H-bond interactions are less pronounced with the higher molar mass APE-2 which has less COOH end groups available for H-bonding with PVP.

The fact that the blends of APE-2 with the lowest molar mass PVP were not fully miscible in compositions of between 30 and 80% of PVP might be explained if we also consider the end-groups of the PVP. It is known that commercial PVP is hydroxyl terminated, because of the involvement of the water as polymerization medium and the presence of hydrogen peroxide.<sup>33,34</sup> This was confirmed by the present authors for PVPK15 and PVPK30 using H NMR. These hydroxyl groups can also form H-bonds with the pyrrolidone groups of PVP, competing with the carboxyl of the APE resins. In the former case, the H-bonds promote intermolecular and intramolecular interactions between the PVP macromolecules (PVP–PVP interactions) lowering the extent of the intermolecular interactions between the PVP and the APE resins. A consequence of PVP–PVP interactions, being more favorable than PVP–APE ones, could be the immiscibility of the hydrophilic polymer with the hydrophobic resin (scheme 1).

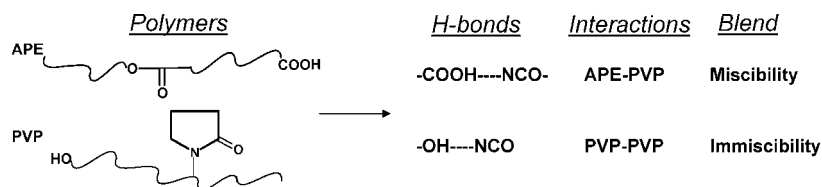
This argument is the most important for the lowest molar mass PVPK15 where the number of OH end-groups is much higher compared to the PVPK30 and PVPK90. As a result, the PVP–PVP interactions are rather significant for the PVPK15 and much less relevant for the higher molar mass PVPK30 and PVPK90. This observation might explain why the miscibility of the APE-2 is enhanced by increasing the  $M_w$  of the PVP: at higher  $M_w$  the number of OH groups in PVP decreases and the PVP–PVP interactions are suppressed, thus the APE–PVP interactions are promoted. Moreover, we have seen that the resin APE-1, which has a smaller molar mass and a higher number of acid end-groups than the APE-2, is miscible at all ratios with the PVPK15. This result also might be explained if we consider that the PVP–APE-1 interactions, due to the higher number of COOH groups, prevail over the PVP–PVP interactions and makes PVP miscible with the APE-1. In other words, the PVPK15 behaves like a more hydrophilic polymer compared to the PVPK30 and PVPK90. In order to promote the miscibility with the APE resin, there are two possibilities: raising the number of COOH groups in APE and/or increasing the molar mass of the PVP.

**CPMAS  $^{13}\text{C}$  NMR Analysis.** CPMAS  $^{13}\text{C}$  NMR spectroscopy and  $^1\text{H}$  NMR relaxometry are powerful tools for studying miscibility and morphology of polymer blends.<sup>35</sup> While  $^1\text{H}$ -to- $^{13}\text{C}$  cross-polarization enhances the NMR signal of the  $^{13}\text{C}$  nuclei, magic angle spinning narrows the intrinsically broad solid-state  $^{13}\text{C}$  NMR resonances, so that chemically different carbon atoms are resolved. Molecular contacts between the components in a highly miscible polymer blend affect the local magnetic fields at the positions of the observed  $^{13}\text{C}$  nuclei, which shows up as  $^{13}\text{C}$  NMR shift or line width changes compared to the homopolymer spectra.<sup>4,15</sup> As shown in Figure 10 such changes are indeed observed. MAS  $^{13}\text{C}$  NMR spectra of PVP–PNI blends show an upfield shift of the carbonyl signals around 175 and 165 ppm (assigned to PVP and PNI, respectively) as a function of PVP content. The fact that the two components in the blend affect each other's  $^{13}\text{C}$  NMR shifts is indicative for short-range interchain contacts and therefore for miscibility at the molecular scale. This result is in agreement with the FTIR spectra, in which, upon mixing the PVP and the APE together, the stretching vibrations of the carbonyls of both polymers shift to higher frequencies.

Polymer miscibility can also be estimated from proton spin–lattice relaxation times in the laboratory frame,  $T_1(^1\text{H})$ , and in the rotating frame,  $T_{1\rho}(^1\text{H})$ . From the  $^1\text{H}$  NMR point of view, polymer materials represent a network of hydrogen nuclei



## Scheme 1. Interactions between PVP and APE End Groups



coupled by magnetic dipole interactions. These dipolar couplings between neighboring hydrogen nuclei lead to so-called spin diffusion of magnetic perturbations in the network. As a result,  $^1\text{H}$  NMR spin-lattice relaxation after an initial perturbation reflects spatially averaged properties of the hydrogen nuclei.<sup>36,37</sup> The averaging length scale depends on various factors, such as the H-H distance, the mobility of the polymer chains, and the actual  $T_1$  and  $T_{1\rho}$  relaxation rates. However, as a rule of thumb for polymers,  $T_{1\rho}$  represents relaxation averaged over a few nanometers, whereas  $T_1$  reflects average NMR relaxation within a sphere of 0.1 to 1  $\mu\text{m}$  in diameter.  $T_1(^1\text{H})$  values of PVPK30 and PNI and their blends were extracted from the decay of the overall proton magnetization  $M(t)$  versus the time  $t$  after the initial perturbation. Table 2 shows the  $T_1(^1\text{H})$  values of PVP and PNI and their blends obtained by nonlinear fitting of  $M(t)$ . For both the homopolymers and their blends, the relaxation curves could be well described by monoexponential decays  $M(t) = M_0 \exp\{-t/T_1(^1\text{H})\}$  with single characteristic decay times  $T_1(^1\text{H})$ . The  $T_1(^1\text{H})$  values of the blends are intermediate between those of the two homopolymers. For a macro-phase separated

blend there would be biexponential behavior with two  $T_1$  components corresponding to the relaxation times of the two homopolymers. However, we observed monoexponential relaxation with relaxation times intermediate between the two homopolymer values. This confirms that the two polymers in the blend are homogeneously mixed at the submicrometer length scale, as consistent with the single glass transition observed with DSC. In general, miscibility at a smaller scale, down to a molecular level, can be investigated by measuring  $T_{1\rho}(^1\text{H})$  relaxation of the homopolymers and their blends. In the particular case of PNI and PVPK30, however, this approach did not work, since the  $T_{1\rho}$  relaxation times of the homopolymers happen to be practically the same,  $T_{1\rho}(^1\text{H}) \sim 14$  ms (Figure 11). As expected from the lack of  $T_{1\rho}$  contrast between PVP and PNI, all PVP-PNI blends show the same  $T_{1\rho}$  relaxation (Figure 11), but this cannot be regarded as prove for miscibility at the molecular scale.

## Conclusions

In this paper, for the first time, blends of the water-soluble poly(*N*-vinyl-2-pyrrolidone) (PVP) with acid functional polyester resins (APE) were studied. According to the DSC results, the two polymers are completely miscible depending on the acid values of the resin and on the  $M_w$  of the PVP.

The nature of the interactions was studied by use of ATR-FTIR spectroscopy. The shifts of the carbonyls of both the PVP and the APE resins to higher frequency (blue shift) upon blending suggests that electric dipole-dipole interactions take place between the two polymers. In addition, the temperature-dependent ATR-FTIR results shows that the broad shoulder of the PVP carbonyl peak at  $1630\text{ cm}^{-1}$  can be ascribed to H-bonds between the carbonyl groups of the PVP and the acid-end groups of the APEs.

The CPMAS  $^{13}\text{C}$  NMR spectra of blends of the acid functional polyester resin of neopentylglycol and isophthalic acid (PNI) with PVPK30 showed systematic changes of the chemical shifts of the PVP and PNI carbonyl resonances as a

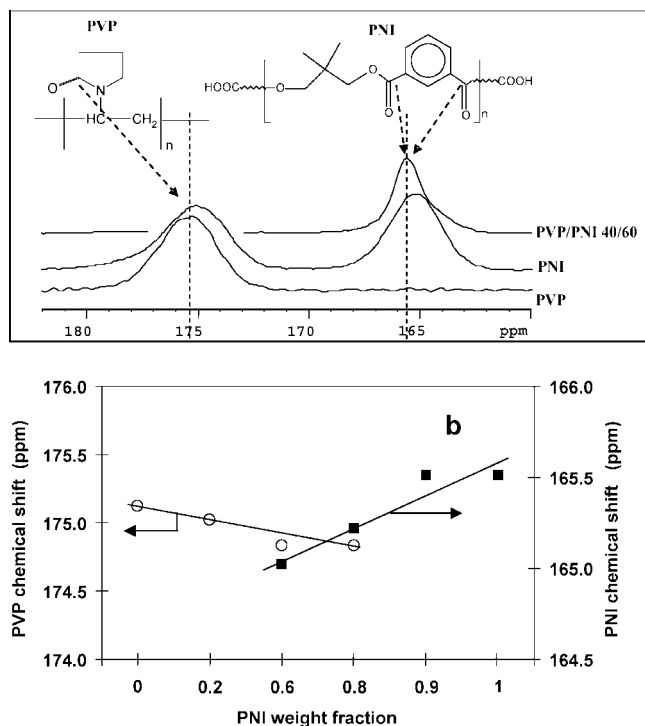


**Figure 10.** (a) carbonyl region of CPMAS  $^{13}\text{C}$  NMR spectra of PVP, PNI and a blend with 60 wt % PNI and (b) PVP and PNI carbonyl shift as a function of PNI content.

**Table 2. Proton  $T_1$  Values for PVPK30/PNI Blends**

PVPK30/PNI	$T_1(^1\text{H})$ (s)
0/100	1.8
20/80	1.7
40/60	1.3
80/20	2.0
100/0	2.7

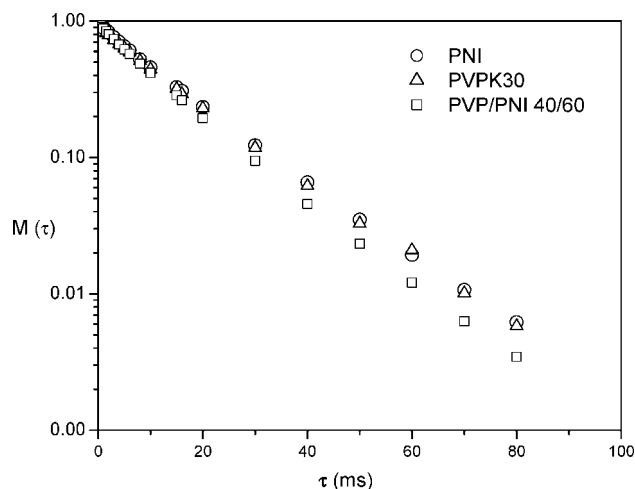


**Figure 11.** Proton  $T_{1\rho}$  relaxation curves for pure PNI, PVPK30 and their blend (40% wt PVPK30) as function of spinlock time,  $\tau_a$  (ms).

result of the mixing. This result confirms that molecular interactions are involved between the two polymers.

The monoexponential spin–lattice relaxation found for PVP, PNI resin and their blends (10, 20, 40, and 80 wt % of PVP) confirms that PVP mixes with the PNI resins at the submicron scale as consistent with the single glass-transition observed with DSC. Due to the coincidental lack of  $T_{1\rho}$ -relaxation contrast between the homopolymers PVP and PNI, it was impossible to obtain information about the miscibility at the nanometer length scale from proton  $T_{1\rho}$  relaxometry.

**Acknowledgment.** This research forms part of the research programme of the Dutch Polymer Institute (DPI), Project No. 422. The authors thank B. Noordover, P. Malanowski, and F. Scaltro (TU/e) for their scientific support.

## References and Notes

- (1) Olabisi O.; Robeson L. M. *Polymer-Polymer Miscibility*; Academic Press: New York, 1979.
- (2) Coleman, M. M.; Serman, C. J.; Bhagwagar, D. E.; Painter, P. C. *Polymer* **1990**, *31*, 1187.
- (3) Nishio, Y.; Haratani, T.; Takahashi, T. *J. Polym. Sci., Part B: Polym. Phys.* **1990**, *28*, 355.
- (4) Zhang, X. Q.; Takegoshi, K.; Hikichi, K. *Polymer* **1992**, *33*, 712.
- (5) Ping, Z. H.; Nguyen, Q. T.; Neel, J. *Makromol. Chem.—Macromol. Chem. Phys.* **1990**, *191*, 185.
- (6) Feng, H. Q.; Feng, Z. L.; Shen, L. F. *Polymer* **1993**, *34*, 2516.
- (7) Cassu, S. N.; Felisberti, M. I. *Polymer* **1997**, *38*, 3907.
- (8) Moskala, E. J.; Varnell, D. F.; Coleman, M. M. *Polymer* **1985**, *26*, 228.
- (9) Eguiazabal, J. I.; Iruin, J. J.; Cortazar, M.; Guzman, G. M. *Makromol. Chem.—Macromol. Chem. Phys.* **1984**, *185*, 1761.
- (10) Deilarduya, A. M.; Iruin, J. J.; Fernandezberridi, M. J. *Macromolecules* **1995**, *28*, 3707.
- (11) Masson, J. F.; Manley, R. S. *Macromolecules* **1991**, *24*, 6670.
- (12) Sionkowska, A. *Eur. Polym. J.* **2003**, *39*, 2135.
- (13) Guo, Q. P. *Makromol. Chem.—Rapid Commun.* **1990**, *11*, 279.
- (14) Dong, J.; Fredericks, P. M.; George, G. A. *Polym. Degrad. Stab.* **1997**, *58*, 159.
- (15) Zheng, S. X.; Guo, Q. P.; Mi, Y. L. *J. Polym. Sci., Part B: Polym. Phys.* **1999**, *37*, 17–2412.
- (16) Neo, M. K.; Goh, S. H. *Polym. Commun.* **1991**, *32*, 7–200.
- (17) Low, S. M.; Goh, S. H.; Lee, S. Y.; Neo, M. K. *Polymer Bull.* **1994**, *32*, 2–187.
- (18) Zhang, G. B.; Zhang, J. M.; Zhou, X. S.; Shen, D. Y. *J. Appl. Polym. Sci.* **2003**, *88*, 4–973.
- (19) Misev, T. A. *Powder Coatings Chemistry and Technology*; Wiley: New York, 1991.
- (20) Senatore, D.; ten Cate, A. T.; Laven, J.; van Benthem, R. A. T. M.; de With, G. *Polym. Mater.: Sci. Eng. Prepr.* **2007**, *97*, 912.
- (21) Hohne G. H. W. F. H. J. In *Differential Scanning Calorimetry a guide for practitioners*; Springer: Berlin, 1996; p 163.
- (22) Koleske, J. V. *Polymer Blends*, Academic: New York, 1978; p 22.
- (23) Garton, A. *Infrared spectroscopy of polymer blends, composites and surfaces*; Carl Hanser Verlag: Munich, 1992.
- (24) Kaplan, D. S. *J. Appl. Polym. Sci.* **1976**, *20*, 2615.
- (25) Hale, A.; Bair, H. E. In *Thermal characterization of polymeric materials*, 2nd ed.; Turi, E., Ed.; Academic Press: San Diego, CA, 1997; Chapter 4, pp 745–886.
- (26) Fox, T. G. *Bull. Am. Phys. Soc.* **1956**, *1*, 123.
- (27) Gordon, M.; Taylor, J. S. *J. Appl. Chem.* **1952**, *2*, 493.
- (28) Macknight, W. J.; Karasz, F. E.; Fried, J. R. In *Polymer Blends*; Paul, D. R., Newman, S., Eds.; Academic Press: New York, 1978.
- (29) Kyu, T.; Ko, C. C.; Lim, D. S.; Smith, S. D.; Noda, I. *J. Polym. Sci., Part B: Polym. Phys.* **1993**, *31*, 1641.
- (30) Rothschild, W. G. *J. Am. Chem. Soc.* **1972**, *94*, 8676.
- (31) He, Y.; Zhu, B.; Inoue, Y. *Prog. Polym. Sci.* **2004**, *29*, 1021.
- (32) He, Y.; Asakawa, N.; Inoue, Y. *Macromol. Chem. Phys.* **2001**, *202*, 1035.
- (33) Washio, I.; Xiong, Y. J.; Yin, Y. D.; Xia, Y. N. *Adv. Mater.* **2006**, *18*, 1745.
- (34) Raith, K.; Kuhn, A. V.; Rosche, F.; Wolf, R.; Neubert, R. H. H. *Pharm. Res.* **2002**, *19*, 556.
- (35) McBrierty, V. J.; Douglass, D. C. *Macromol. Rev., Part D: J. Polym. Sci.* **1981**, *16*, 295.
- (36) Schimdt-Rohr, K.; Spiess H. W. *Multidimensional solid-state NMR and polymers*; Academic Press: London, 1994.
- (37) Magusin, P. C. M. M.; Mezari, B.; van der Mee, L.; Palmans, A. R. A.; Meijer, E. W. *Macromol. Symp.* **2005**, *230*, 126.

MA800017T